

Determination of the hot intracluster gas temperature from submillimeter measurements

E. Pointecouteau , M. Giard and D. Barret

Centre d'Etude Spatiale des Rayonnements, 9 avenue du Colonel Roche, BP-4346 31029 Toulouse, France.

Received ; accepted

Abstract.

Measurements of the Sunyaev-Zeldovich (hereafter SZ) distortion of the cosmic microwave background can give interesting physical informations on clusters of galaxies, provided that the electronic temperature of the gas is known. Previous attempts to do so have used the electronic temperature determination obtained from the X-ray spectra. However, if the intergalactic gas is not homogeneous, the X-ray emission will trace the denser component, and the temperature determination may not be relevant for the lower density gas which is dominating the SZ measurements. Moreover, the X-ray brightness decreases very rapidly with the distance, which is not the case for the SZ effect. Distant clusters might be detected from SZ measurements, whereas they are inaccessible to X-ray observations. For these reasons, we have investigated the possibility to derive the electronic temperature of the gas from the SZ measurements in the submillimeter range ($\lambda \sim 300 - 600 \mu\text{m}$). We show that given the sensitivities of the future submillimeter space missions Planck Surveyor and FIRST, the electronic temperature of massive clusters ($Y_{\text{center}} = 3 \times 10^{-4}$) can be determined with an accuracy ranging from 1 to 4 keV depending on its distance and the data available.

Key words: cosmic microwave background – intergalactic medium – galaxies: clusters: general

1. Introduction

The intergalactic medium is a strong source of diffuse X-ray radiation by free-free emission (Jones & Forman 1984). It is observed at submillimeter wavelengths too, via the Sunyaev-Zeldovich (hereafter SZ) effect: a spectral distortion of the Cosmic Microwave Background (hereafter CMB) due to the interaction of the electrons of the hot ionized gas with the photons of the CMB (Zel'dovich & Sunyaev 1969, Sunyaev & Zeldovich 1972). If the electronic temperature is determined from X-ray data, together with a model of the gas distribution, SZ data allow to derive the Compton optical depth (τ) of the intergalactic gas. This parameter directly provides the gas mass, if it is integrated over solid angles. The association of X-ray and SZ data allows to estimate the Hubble constant, H_0 , independently of the usual standard candles

methods (see Holzapfel et al. 1997 for instance). The peculiar velocity of several clusters can also be derived from the Doppler effect, so that it should be possible to detect the large scale gravitational field which is produced by the dark matter.

An important feature of the SZ brightness is that it is an absorption effect on the CMB, which intensity is independent of z (if no evolution of the cluster is assumed). On the contrary, the cluster's X-ray surface brightness decreases with respect to the usual $(1+z)^{-3}$ expansion factor and with respect to an additional exponential factor, $\exp(-E(1+z)/kT_e)$, which becomes important for very distant clusters.

In this paper, we investigate how the gas cluster temperature can be recovered from the SZ measurements themselves. In section 2, we present a simple Monte-Carlo method which allows to obtain the exact shape of SZ spectra, taking into account the temperature dependence which is ignored in the usual analytical expression. We emphasize the spectral effect due to the gas temperature which shows up in the submillimeter domain. In section 3 we quantify the error on the determination of the gas temperature using SZ measurements only, considering limitations of the instruments sensitivities and of the various foreground and background emissions.

2. Exact calculations of the SZ effect

The frequency dependency of the SZ effect is usually approximated by a solution of the Kompaneets equation (Kompaneets 1972) which is a second order approximation of the Boltzmann equation (Rybicki & Lightman 1979). This solution needs:

$$\left. \frac{\Delta I_\nu}{I_\nu} \right|_{th} = y f(x) \quad (1)$$

for the thermal effect,

$$\left. \frac{\Delta I_\nu}{I_\nu} \right|_{kin} = -\frac{v_p \tau}{c} a(x) \quad (2)$$

for the kinetic effect,

$f(x)$ and $a(x)$ are analytic functions of the dimensionless frequency:

$$x = \frac{h\nu}{kT_r} \quad (3)$$

y is the Comptonization parameter of the cluster:

Send offprint requests to: E. Pointecouteau, pointeco@cesr.fr

$$y = \frac{k T_e}{m_e c^2} \tau \quad (4)$$

T_e is the electronic temperature of the intergalactic gas, v_p is the peculiar velocity of the cluster, τ is the Compton optical depth of the intergalactic gas. $T_r = 2.726\text{K}$ is the CMB temperature.

Photons of the CMB are scattered from low frequencies to higher frequencies. The cross-over frequency is around $\nu = 217\text{ GHz}$ (e.g. $\lambda = 1.38\text{ mm}$).

In case of millimeter and submillimeter SZ data, the analytic approximation yield to analysis errors. Indeed, the electronic temperature level implies weakly relativistic velocities for the electrons. A few authors have worked on the relativistic corrections of the SZ effect (Wright 1979, Fabbri 1981). Most recently, Rephaeli (1995) has compiled previous works to develop a semi-analytical treatment of the SZ effect and Stebbins (1997), Challinor & Lassenby (1997) and Itoh et al. (1997) have extended analytically the Kompaneets equation. However, the exact SZ spectra can be obtained using a simple Monte-Carlo method which numerically integrates the transfer equation:

$$\frac{\partial I_\nu}{\partial s} = n_e \int d\beta \int d\Omega p_e(\beta) \frac{d\sigma}{d\Omega} [I_\nu(\nu_1) - I_\nu(\nu)] \quad (5)$$

where $p_e(\beta)$ is the velocity distribution of the electrons, $\beta = \frac{v}{c}$, $\frac{d\sigma}{d\Omega}$ is the differential scattering cross section, I_ν is the intensity of the radiation at the frequency ν (before scattering) and ν_1 (after scattering), n_e is the density of the electrons.

The frequency shift of the photons is given by:

$$\frac{\nu_1}{\nu} = \frac{1 - B}{1 + B_1 + \frac{h\nu}{m_e c^2} (1 - \cos \alpha)} \quad (6)$$

where $B = \beta \cos \theta$ and $B_1 = \beta \cos \theta_1$ and $\cos \alpha = \cos \theta \cos \theta_1 + \sin \theta \sin \theta_1 \cos(\phi - \phi_1)$, (θ, ϕ) and (θ_1, ϕ_1) are the angles between the electron's and the photon's directions of propagation, respectively before and after the scattering.

The exact differential cross-section has to be used (Podzniakov, Sobol & Sunyaev 1983):

$$\frac{d\sigma}{d\Omega} = \frac{r_e^2}{2} \frac{1 - B}{\gamma^2 (1 + B_1)^2} (1 + [1 - \frac{1 - \cos \alpha}{\gamma^2 (1 - B)(1 - B_1)}]^2) \quad (7)$$

$r_e = e^2 / m_e c^2$ is the classical radius of the electron and $\gamma = (1 + \beta^2)^{-1/2}$ is the Lorentz's factor.

As shown on Fig. 1, the spectra that we obtained are in accordance with those calculated by Rephaeli (1995). Those spectra can be obtained from our anonymous ftp site (<ftp.cesr.fr/pub/astrophysique/sz/>). We will show hereafter that the SZ dependency on T_e can be used to derive the intracluster gas temperature from submillimeter data (see Fig. 1).

3. Determinations of the electronic temperature

In a few years the Planck Surveyor and FIRST missions will detect the SZ effect with a very good sensitivity. It is likely that new distant clusters will be identified with SZ data and that these clusters will remain out of reach for the X-ray and/or optical telescopes. In the following, we discuss the two ways of determining the electron temperature for galaxy clusters from X-ray or SZ data.

3.1. Precision of X-ray determinations

Using the XSPEC software (Arnaud 1996) we simulated a 25 kilosecond ASCA (GIS2) observation of a galaxy cluster with the following spectral parameters: Bremsstrahlung temperature (T_e) of 8 keV, an unabsorbed 1-10 keV flux of $6 \times 10^{-11} \text{ ergs s}^{-1} \text{ cm}^{-2}$ corresponding to a rich cluster with $0 < z < 0.2$ observed through a column density of $10^{21} \text{ H atoms cm}^{-2}$. For such an observation, T_e is recovered with an error of typically 0.5 keV at 68% confidence level. These errors are consistent with those derived from actual observations (David 1993). Given the ASCA energy range (0.1-10 keV), the error on T_e should increase with T_e . This is simply because as T_e increases the cutoff in the Bremsstrahlung spectrum moves at higher energies, and approaches or even exceeds the high energy threshold of the instrument where its sensitivity drops sharply. Consequently, fitting the spectrum will tend to underestimate T_e . This is a major limiting factor which is primarily related to the energy coverage of the instrument. This will also apply to future instruments, like XMM, although their sensitivities are much better than ASCA. For instance simulating an ASCA observation with the same input spectrum as above but with $T_e = 12 \text{ keV}$, the fit recovers T_e as $10.9 \pm 0.9 \text{ keV}$ (90% confidence) barely consistent with the input value. Obviously the recovered T_e and associated errors via X-ray observations depends also on the input flux which has to be compared with the instrument detection sensitivity. As the X-ray flux at earth decreases sensitively with the redshift (e.g. $z \geq 1$), for distant clusters the accuracy in determining T_e will also decrease. For instance, Hattori et al. (1997) fitted the ASCA data of the AXJ2019+1127 X-ray cluster to $z = 0.94$ and $T_e = 8.6^{+4.2}_{-3.0} \text{ K}$.

In the case of an inhomogeneous intracluster gas, if we considered the temperature-density correlation, a T_e determination via X-ray emission ($\propto \int n_e^2(l) dl$) may miss a low density component of the gas, so that an independent temperature determination, via SZ measurements (mostly sensitive to a low component, e.g. $\propto \int n_e(l) dl$) is also interesting.

3.2. Temperature determination with Planck and FIRST

In the following, we have simulated SZ measurements of a rich cluster performed with Planck and FIRST. The photometric bands used are those of the HFI for Planck, PHOC and SPIRE for FIRST. Their characteristics are summarized in Table 1. They are taken from the COBRAS/SAMBA Phase A report concerning Planck (except for the additional bolometer channel at 100 GHz). Concerning FIRST, we have assumed that the noise level used is the quadratic sum of the photon noise, $NEP_{phot} = h\nu (\frac{S\Omega}{\lambda^2} \Delta\nu \epsilon \eta n (1 + \epsilon \eta n))^{1/2}$ and the detector noise $NEP_{det} = 3 \times 10^{-17} \text{ W}/\sqrt{\text{Hz}}$. $S\Omega/\lambda^2 = 1$ at the diffraction limit, $\Delta\nu/\nu \simeq 0.3$, $\epsilon = 0.03$ is the telescope emissivity, $\eta = 0.5$ is the system response (including transmission and detector efficiency), $n = 2/(e^{(\frac{h\nu}{kT_{tel}})} - 1)$ is the photon phase space occupation number for the telescope thermal emission, $T_{tel} = 80 \text{ K}$ (satellite at L_2 Sun-Earth Lagrangian point.). The wavelengths of the FIRST lower frequency channels have been adjusted to the Planck higher frequency bands.

We estimate the precision of the temperature determination by repetitive least square fits on simulated submillimeter and millimeter data: Planck alone or Planck plus FIRST combination. We take into account both the instrumental noise and the contaminating sky emissions: galactic dust, free-free, syn-

	FIRST				PLANCK					
ν (GHz)	1765	1200	857	545	857	545	353	217	150	100
θ (arcmin)	4.5 ⁽¹⁾	4.5 ⁽¹⁾	4.5 ⁽¹⁾	4.5 ⁽¹⁾	4.5	4.5	4.5	4.9	7.4	10.6
NEB (10^{-2} MJy/sr/ $\sqrt{\text{Hz}}$)	11.0 ⁽¹⁾	8.1 ⁽¹⁾	6.2 ⁽¹⁾	4.3 ⁽¹⁾	6.1	5.9	2.9	2.6	1.4	1.0
rms I_{DUST} (10^{-2} MJy/sr)	63.	44.	22.	6.4	22.	6.4	1.5	0.27	0.06	0.01
rms I_{ULIRG} (10^{-2} MJy/sr)	0.61	0.59	0.45	0.021	4.8	2.2	0.7	0.12	0.01	0
rms I_{CMB} (10^{-2} MJy/sr)	0	0	0.01	0.47	0.01	0.47	2.5	3.9	3.1	1.9
rms $I_{ff+synch}$ (10^{-2} MJy/sr)	0.034	0.039	0.041	0.046	0.041	0.046	0.051	0.058	0.066	0.074
$f_{dill}(z=0.1)$	0.87	0.87	0.87	0.87	0.87	0.87	0.87	0.85	0.74	0.62
$f_{dill}(z=1)$	0.43	0.43	0.43	0.43	0.43	0.43	0.43	0.41	0.28	0.2

Table 1. Characteristics of the Planck Surveyor’s and the FIRST’s passbands used. The Noise Equivalent Brightness (e.g. NEB) is given for the nominal beams for Planck and for a virtual beam for FIRST ⁽¹⁾. The rms contribution of the backgrounds and foregrounds are given for the beam used (see caption of Fig. 1 and text). Dilution factors applied to $Y_{center} = 3 \times 10^{-4}$ are given for redshifts $z = 0.1$ and $z = 1$ and for a cluster with $R_c = 0.3$ Mpc and $\Omega_{tot} = 0.3, H_0 = 70$ km/Mpc/s.

⁽¹⁾ A virtual beam of 4.5 arcmin (e.g. the Planck submillimeter beam) is used in simulations. It will be obtained by summation of adjacent sky pixels. The NEB in each bands is the sum of photon noise and detector noise, as determined in section 3.2.1, modified by a factor equal to the ratio of the diffraction limit beam to virtual beam diameters

chrotron, Ultra-Luminous InfraRed Galaxies (ULIRGs), and CMB. We did not attempt to determine the velocity through the kinetic effect since it is spectrally identical to the primary CMB and has already been extensively studied (see Haehnelt & Tegmark 1996 and Aghanim et al. 1997).

3.2.1. Simulation of clusters observations

We simulate a massive cluster, $Y_{center} = 3 \times 10^{-4}$, with isothermal β density gas profile, $T_e = 8\text{keV}$, $\beta = 2/3$, $R_c = 0.3$ Mpc, $n_0 = 1.9 \times 10^{-2} \text{cm}^{-3}$. We take into account the dilution of the cluster SZ emission in the instrumental beam by proper integration of the SZ profile over the beam (we assume the density cutoff at $15 R_c$). Concerning the FIRST channels we use with a virtual beam equal to the Planck submillimeter beam (4.5 arcmin) which will be obtained by the summation of adjacent sky pixels. The surface brightness noise level (NEB) is correspondingly improved from the diffraction limit value by a factor equal to the ratio of the diffraction limit beam to the virtual beam. The signal is then correctly integrated over the finite bandpass of the instruments.

We then add the following astrophysical contributions:

- A dust signal with rms level $I_{100\mu} = 0.3$ MJy/sr, value which is not exceeded on 19% of the whole sky (This percentage is determined from an all sky map of the rms $100 \mu\text{m}$ fluctuations calculated in bins of $0.7^\circ \times 0.7^\circ$ from the ISSA IRAS maps). A spectral characteristics $T = 17.5\text{K}$, $n = 2$, typical of high latitude clouds (Boulanger et al. 1996). The variability of the dust spectrum is taken into account by introducing a random fluctuation in the spectral index. This is fixed to 10% rms of the average value ($n = 2$), in accordance with measurements of the 2 meter submillimeter stratospheric telescope PRONAOS on high latitude galactic cirrus (Bernard et al., in preparation).

- Fluctuations of the integrated contribution from the background ULIRGs. Their rms level is integrated from the number counts of Guiderdoni et al. (1997). The flux limit is set such that the probability to find a source brighter than that limit within the beam is smaller than 10% for the Planck’s bands. For FIRST, considering the high angular resolution available, we assume that all sources above the 3σ noise level are detected

and subtracted before summation in the 4.5 arcmin virtual beam.

- Fluctuations of the primary CMB at a rms level of $\Delta T/T = 30 \times 10^{-6}$ (e.g. $\Delta v_p \simeq 500$ km/s for our cluster).

- free-free and synchrotron: Their level and spectral behaviour are taken from the COBE determination (Bennett et al. 1992): $7\mu\text{K}$ rms free-free at 53 GHz with spectral index $n = -0.16$, $4\mu\text{K}$ rms synchrotron at 53 GHz with spectral index $n = -0.9$. (The COBE measurement has been extrapolated to sub-degree angular scales assuming l^{-3} , Bersanelli et al. 1996).

A random instrumental noise with rms level as in Table 1 is then added to the astrophysical signal. Finally, a 1% relative error is randomly added to all bands to take into account the band to band calibration uncertainty.

The different emissions and noise levels are shown in Fig. 2 together with the instrumental band positions.

3.2.2. Restoration of the cluster’s parameters

We fit a five parameters model to the simulated multi-band measurements. This model is the sum of : SZ thermal effect (T_e, Y_{center}), primary CMB ($\Delta T/T$) and dust (C_d, n). C_d and n are respectively the level and spectral index of the dust. The model also take into account the integration over different spectral bands.

The errors on the restored parameters are estimated from the statistics of the multiple simulations and fits. The ULIRGs are not explicitly included in the separation because their spectrum is very close to galactic dust spectrum, however they are partly taken into account through the variable spectral index of the fitted dust.

4. Results and discussion

Due to the likely curvature of the universe, a massive cluster as the one considered in the previous section ($r_c > 0.3$ Mpc), will never show a SZ profile having a width at half maximum less than 2 arcmin. The integration time (~ 10 s) is the main limiting factor concerning the use of the Planck survey to measure the SZ effect with a high accuracy. Actually, this should

be overcome by the FIRST telescope. Whatever are the missions final concepts and observing strategies, data from the two satellites will be available in a few years, and will provide a unique tool to study distant clusters of galaxies via precise measurements of the submillimeter SZ effect.

The accuracy on the determination of T_e is strongly dependent on the integration time. The FIRST Deep survey, a foreseen key program (Beckwith et al. 1993), is expected to cover 100 square degrees on the sky, for a total time of 2×10^6 seconds that corresponds to an integration time of 500s per position, which is the value that we will use in the following. According to the Planck's mission observing strategy, some parts of the sky will be observed with an integration time a factor of 10 higher than the nominal time. (about 100 squared degrees on the sky.).

We restore the gas temperature for these two integration times in the cases of Planck alone and the FIRST/Planck data combination. For Planck alone, effective beams are all fixed to 10.6 arcmin (the 3mm beam of Planck) to obtained a better sensitivity.

Results are summarized in Table 2.

The accuracy on the estimation of the SZ parameters and the number of clusters that will be detectable depends on the observing strategy. A first one would be to search for rich clusters in the FIRST deep survey fields, completed by the corresponding positions of the Planck survey. One can expect that part of the FIRST deep survey will be performed in a region where Planck has a higher integration time per pixel (P2/F case in Table 2). The precision on the temperature determination is in this case of 1.2 keV ($z = 0.1$) to 3.9 ($z = 1.$). Massive distant clusters can be identified in the FIRST data as positive extended excesses at the larger wavelengths, after removal of the dust component. (The dust contamination should not be a problem since the deep survey field will be selected among the best galactic windows).

A second strategy will consist of a search for rich clusters in the Planck survey, completed by pointed observations with FIRST. The distant rich clusters will show almost no spatial extension in the Planck survey ($FWHM_{SZ} \simeq 3.5\theta_c \simeq 2.2$ arcmin at $z = 1$) and will be recognized among the faint clusters detected in the Planck survey, because they will have no or only faint X-ray counterparts. Actually, massive clusters (e.g: $y > 3. \times 10^{-4}$) will be detectable in the Planck survey data at all redshifts: the most extreme dilution factor for such a cluster is about 0.18 (10.6 arcmin beam) and the instrument sensitivity to SZ effect is of order 1.34×10^{-6} (no dilution). For each cluster, depending on the detector array size, a five arcmin field on the cluster (plus comparison field) can be covered with FIRST within a few hours of observation. The precision on the temperature determination will be of order 1.2 to 1.4 keV for a cluster at $z = 0.1$, depending on the Planck integration time on this cluster. For very distant clusters the dilution is important and the precision is limited to ~ 4 keV due to the contamination of the infrared background galaxies. This result, which is comparable to the precision of the current X-ray determinations (Hattori et al. 1997), could be improved by cleaning properly the emission in the Planck bandpass from the infrared galaxies contamination.

Depending on the age of the universe, its geometry and the epoch of cluster formation, there may be a few or a large number of distant rich clusters (Oukbir & Blanchard 1997). Al-

	ΔT_e (keV)			
ΔT_e (keV)	P1	P2	P1/F	P2/F
$z=0.1$	3.1	2.2	1.4	1.2
$z=1.$	-	4.2	4.3	3.9

Table 2. 1σ statistical error (keV) on the determination of the gas temperature (8 keV cluster) for different configurations. For Planck alone, P1: nominal integration time. P2:10 \times nominal integration time. For Planck/FIRST, P1/F: Planck's nominal integration time and First deep survey (DS) for FIRST. P2/F: Planck 10 \times nominal time and First deep survey

though cosmological standard models (CDM and $\Omega \simeq 1$) favour the formation of rich structures only at a recent time, and seem to be supported by the X-ray cluster's distribution at $z < 0.5$ (Bartlett & Silk 1994, Luppino & Gioia 1995), several detections of galaxies and structures have been reported at very high z ($1 < z < 5$): Pascarelle et al. (1996), Malkan et al. (1996), Le Fevre et al. (1996) and Dey et al. (1998) at optical wavelengths, the X-ray detection of AXJ2019+1127 by Hattori et al. (1997) at $z=0.94$. Most unexpected have been the detections by Jones et al. (1997) and Richards et al. (1997) of negative decrements at centimeter wavelengths in the direction of distant quasars. These decrements can be attributed to massive clusters at $z > 1$, unobservable at other wavelengths.

Korolyov et al. (1986) were the first to write that it is easier to detect high redshift clusters of galaxies in microwave spectral band than in X-rays. If this is confirmed, it means that a fairly large number of rich clusters may be detectable in the Planck survey and selected on the basis of low dust contamination and faint (or no) X ray counterparts for observations with FIRST.

Acknowledgements.

We thank N. Aghanim, F.X. Desert and F. Bouchet for their very helpful suggestions. We are very grateful to the referee, R. Sunyaev, for his fruitful comments.

References

- Aghanim, N., et al., 1997, A&A, 325, 9
- Arnaud, K.A., 1996, Astron. Data Analysis Software and Systems V, eds. Jacoby G. and Barnes J., p17, ASP Conf. 101.
- Bartlett, J.G., Silk, J., 1994, ApJ 423, 12
- Beckwith, S., et al., 1993, FIRST Red book, ESA report
- Bennett, C., et al., 1992, ApJ, 391, 466
- Bersanelli, M. et al., 1996, COBRA/SAMBA ESA report
- Boulanger, F., et al., 1996, A&A, 312, 256
- Challinor, A., Lasenby, A., 1997, astro-ph/9711161
- David, L.P., et al., 1993, ApJ 412, 479
- Dey, A., et al., 1998, astro-ph/9803137
- Fabbri, R., 1981, A&SS 77, 529
- Guiderdoni, B., et al., 1997, MNRAS, 295, 877
- Hattori, M., et al., 1997, Nat, 388, 146
- Haehnelt, M., G., Tegmark, M., 1996, MNRAS, 279,545
- Holzappel, W., L., et al. , 1997, ApJ, 480, 449
- Itoh, N., Kohyama, Y., Nozawa, S., 1997, astro-ph/9712289
- Jones, C., Forman, W., 1984, ApJ 276,38
- Jones, M.E., et al., 1997, ApJ, 479, L1

- Kompaneets, A.S., 1957, Sov. Phys.-JETP, 4, 730
 Korolyov, V.A., Sunyaev, R.A., Yakubtsev, L.A., 1986, Sov. Astron. Letters, 12, 141
 Le Fevre, et al., 1996, ApJ, 471, L11
 Luppino, G. A., Gioia, I., M., 1995, ApJ, 445, L77
 Malkan, M., A., Teplitz, H., McLean, I., S., 1996, ApJ, 468, L9
 Oukbir, J., Blanchard, A., 1997, A&A, 317, 1
 Pascarelle, S., et al., 1996, ApJ 456, L21
 Podzniakov, L.A., Sobol, I.M. and Sunyaev, R.A., 1983, Sov. Scientific Review-A&SS, Sunyaev-Hardwood Academy Publishers, New York, vol 2, p 189
 Rephaeli, Y., 1995, ApJ 445, 33
 Rybicki, G.B., Lightman, A.P., 1979, "Radiative Process in Astrophysics", New York: Wiley & Sons
 Richards, E., et al, 1997, AJ 113, 1475
 Stebbins, A., 1997, astro-ph/9709065
 Sunyaev, R.A., Zeldovich, Ya.B., 1972, Comments Astrophys. Space Phys., 4, 173
 Wright, E.L., 1979, ApJ 232, 348
 Zeldovich, Ya.B., Sunyaev, R.A., 1969, Ap&SS 4, 301

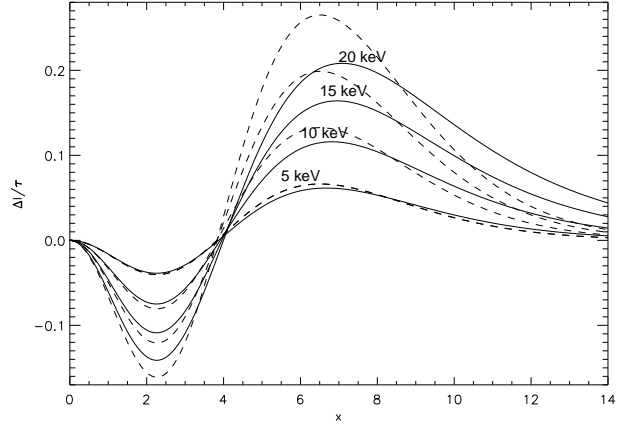


FIG. 1. Comparison of the SZ spectra obtained using the analytical approximation (dotted lines) and those obtained using the exact Monte Carlo calculation (solid lines). Spectra are plotted for clusters with 5, 10, 15 and 20 keV temperature (in units $(hc)^2/[2(kT_e)^3]$).

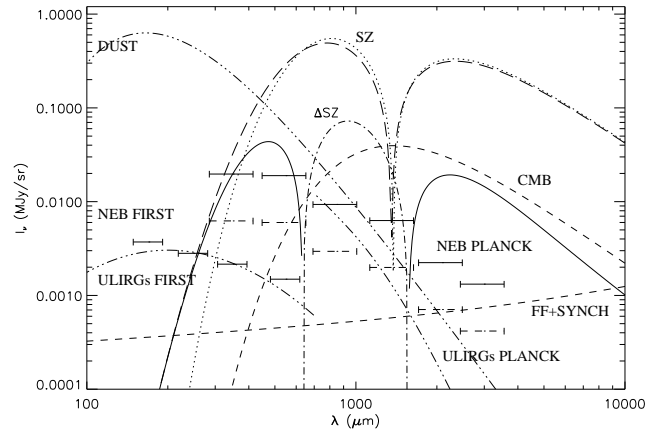


Fig. 2. The temperature effect in the thermal SZ effect (ΔSZ =difference between exact and approximation calculation): solid line for the positive part and dotted-dashed line for the negative part. The exact SZ effect (long dash line) and the analytical approximation (dotted line) are overplotted. ($T_e = 8$ keV, $Y_{center} = 3 \times 10^{-4}$). Other contributions have been plotted: The CMB at the level of $\Delta T/T = 30 \times 10^{-6}$, the galactic free-free plus synchrotron emission respectively normalized at the level of $7\mu K$ and $4\mu K$ at 53 GHz (dashed lines). The galactic dust (with $T_d = 17.5$ K, $n = 2$ and normalized to 0.3 MJy/sr at $100 \mu m$) and the background infrared galaxies beam to beam fluctuations (3 dot-dashed lines). (The background galaxies fluctuations are plotted as two curves, for the Planck and for the FIRST channels, as described in the text.). Horizontal bars represent the Planck and the FIRST sensitivities levels. (Dashed bars for the high sensitivity regions of the Planck survey.)